2002

Low-frequency Variations in Global Mean Sea Level: 1950–2000

D. P. Chambers
University of Texas at Austin, donc@usf.edu

C. A. Mehlhaff
University of Texas at Austin

T. J. Urban
University of Texas at Austin

D. Fujii
University of Texas at Austin

R. S. Nerem
University of Colorado at Boulder

Low-frequency variations in global mean sea level: 1950–2000

D. P. Chambers, C. A. Mehlhaff, T. J. Urban, and D. Fujii
Center for Space Research, University of Texas at Austin, Austin, Texas, USA

R. S. Nerem
Colorado Center for Astrodynamics Research, University of Colorado at Boulder, Boulder, Colorado, USA

Received 3 August 2001; revised 8 November 2001; accepted 16 November 2001; published 17 April 2002

[1] Low-frequency variability in global mean sea level (GMSL) is studied for the period 1950–2000 by interpolating sparse tide gauge data to a global grid using empirical orthogonal functions (EOFs) of sea level variability determined from TOPEX/Poseidon (T/P) altimeter data. Results are based on data with long-term trends removed. The fact that the results do not have secular trends is an artifact of the analysis and should not be interpreted as an indication that sea level is not rising. The EOF reconstruction technique is discussed, and the resulting GMSL time series is compared to GMSL time series from Geosat and T/P altimetry and proxy GMSL time series estimated from global sea surface temperature data. The error assessment suggests the accuracy of the GMSL time series reconstructed from the tide gauge data is 2–4 mm RMS for a 1 year running mean smoothing and about 1 mm for a 5 year running mean smoothing. Several El Niño/La Niña events are evident in the GMSL, as well as significant low-frequency variability at a 10–12 year period. GMSL appears to have been generally lower than normal in the late 1960s, throughout the 1970s, and in the 1980s. GMSL appears to have been generally higher than normal in the late 1950s and early 1960s and in the early 1980s and has been rising throughout the 1990s, when T/P is observing. The implication of the low-frequency signals on the determination the secular rate of GMSL from satellite altimetry is discussed. *INDEX TERMS:* 4556 Oceanography: Physical: Sea level variations; 4215 Oceanography: General: Climate and interannual variability (3309); 1640 Global Change: Remote sensing; 1694 Global Change: Instruments and techniques; *KEYWORDS:* mean sea level, TOPEX/Poseidon, empirical orthogonal functions, tide gauge

1. Introduction

[2] The record of sea level from tide gauges over the past 70–100 years clearly shows a rise in the sampled mean sea level at a rate of between 1 and 2 mm yr^{-1} [e.g., *Church et al.*, 2001; *Douglas*, 2001]. Although the tide gauge record is long at some sites, it does not represent a homogeneous sample of the global oceans. Most gauges with long records tend to be in the Northern Hemisphere and along coastlines. The method for determining the long-term secular rate of sea level rise has been to calculate the local rate at selected tide gauges after applying a model for glacial isostatic adjustment (GIA) and then to average these rates to obtain a global average. Using this method, it is impossible to determine global mean variability at periodic frequencies. It is also assumed that the relatively few sites adequately sample the global mean sea level (GMSL) average rate over the past 100 years or so.

[3] A better measurement of GMSL variations can be made with satellite altimetry since a satellite samples nearly all of the Earth's oceans typically every 10–35 days depending on the orbit configuration. Measurements have been made regularly (with a short gap) since 1985 [*Born et al.*, 1986; *Tapley et al.*, 1992; *Wagner and Cheney*, 1992; *Nerem*, 1995; *Minster et al.*, 1995; *Cazenave et al.*, 1998; *Nerem et al.*, 1999]. The longest continuous record is that made by the TOPEX/Poseidon (T/P) mission, which has been observing the GMSL since September 1992 [*Fu et al.*, 1994]. Data from the T/P mission have increased our knowledge of the spatial and temporal variability of sea level change significantly. For instance, we now know that El Niño-Southern Oscillation (ENSO) events cause large deviations in GMSL [*Nerem et al.*, 1999], that there are significant annual and interannual variations caused by thermal and water mass variations [*Chen et al.*, 1998; *Minster et al.*, 1999; *Chambers et al.*, 2000], and, perhaps more importantly, that the sea level change is not uniform spatially [*Nerem*, 1995; *Hendricks et al.*, 1996; *Nerem et al.*, 1999].

[4] Interannual and low-frequency signals in sea level variability can have significant effects on the recovery of secular trends in short records [*Douglas*, 2001]. *Nerem et al.* [1999] estimated one would need at least 10 years of continuous altimeter coverage to resolve a 2 mm yr^{-1} secular trend with an accuracy of 0.5 mm yr^{-1} in the presence of ENSO variability. However, the study did not model variations with periods longer than 5–7 years because at the time it was unclear if there were significant low-frequency fluctuations in GMSL even though there are clearly such signals in many tide gauge records (e.g., Figure 1).

[5] In addition to the importance of understanding low-frequency GMSL variability on the determination of long-term secular trend, the signal is of interest to studies of climate change. Because GMSL change is related to both steric and water mass variations, even small variability in the GMSL can be indicative of rather significant changes in either the ocean heat storage or water storage. Simply averaging available tide gauge records will not provide a reasonable measure of interannual and low-frequency variation, because of the sampling. For instance, a global average of the tide gauge data from 1993 to 1998 (processed as described in section 2) shows a much larger seasonal variation than that observed by T/P during the same interval (Figure 2). The tide gauge average is computed as an unweighted mean of all data for a particular month. The explanation for the discrepancy is the fact that the tide gauge data are predominantly in the Northern Hemisphere, and so there is no averaging of the out of phase seasonal signal in the Southern Hemisphere, which also has a smaller

0148-0227/02/2001JC001089

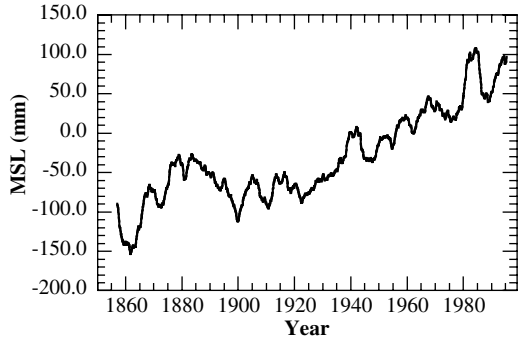

Figure 1. Sea level anomalies from the tide gauge in San Francisco. Data have been smoothed with a 5 year (60 month) running mean boxcar filter.

amplitude. However, even if the seasonal signal is removed from the tide gauge data, the global average still does not measure the same variability as observed by T/P (Figure 2).

[6] Clearly, a global sampling of sea level data is needed in order to resolve the true low-frequency variability in GMSL. Since the altimeter record at best only goes back to 1985, other methods must be used to estimate global grids or approximate a global sample. Several authors have detailed methods to use information contained in global empirical orthogonal functions (EOFs) to estimate better the true global average of sparse data sets. *Shen et al.* [1994] used EOF modes to average optimally sparse sea surface temperature (SST) data. *Smith et al.* [1996] used a least squares fit of EOFs to SST data in order to reconstruct global grids of SST, while *Shriver and O'Brien* [1995] applied a similar method to wind stress. *Kaplan et al.* [1997, 2000] used EOFs as basis functions in an optimal interpolation of SST and sea level pressure using a Kalman filter. *Cane et al.* [1996] used a similar reduced space Kalman filter to assimilate tropical Pacific tide gauge data into an ocean circulation model. All studies found significant improvement in the determination of large-scale interannual and low-frequency variability.

[7] In this paper we utilize EOFs as described by *Smith et al.* [1996] to reconstruct global grids from tide gauge data for the period 1950–1998. EOF modes determined from T/P altimetry will be utilized. The GMSL will be computed from the reconstructed grids and compared with that from T/P and Geosat altimetry, as well as a proxy sea level measurement from SST data. The reconstruction method will be summarized, and the process to compute the proxy sea level from SST will be discussed. An analysis of the estimated low-frequency variations in GMSL will be presented, and the implication of such variability on determining the secular rate of GMSL from satellite altimetry will also be discussed.

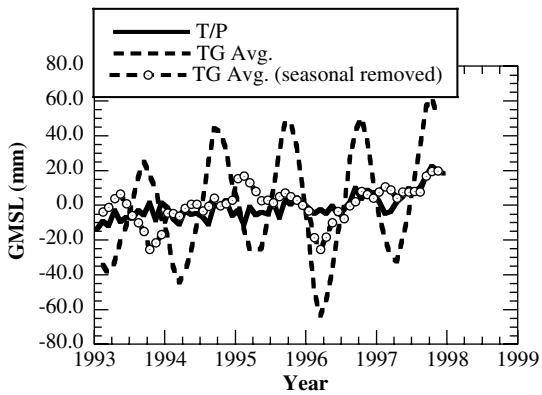

Figure 2. Sea level anomalies from T/P, average of tide gauge data, and average of tide gauge data with seasonal variations removed.

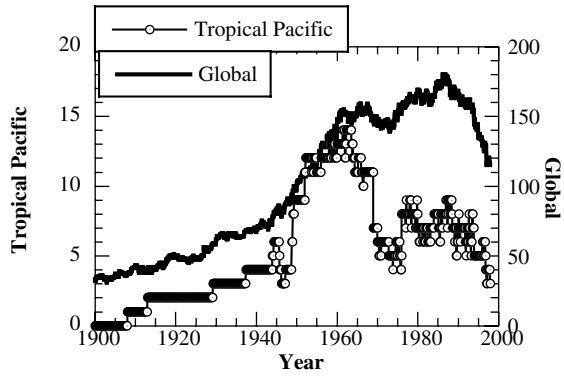

Figure 3. Number of grids with tide gauge observations for global ocean (right scale) and tropical Pacific (left scale).

2. Data Processing

[8] T/P altimeter data come from the Merged Geophysical Data Records B (MGDR-B) release for cycles 10–231 from the NASA Jet Propulsion Laboratory [*Benada*, 1997]. These data include improved orbits and geophysical corrections, including the ocean tide, pole tide, and sea state bias. All standard corrections are applied, and data are edited according to flags as recommended. All data are corrected for a drift in the TOPEX Microwave Radiometer as recommended by *Keihm et al.* [2000]. An inverted barometer (IB) correction has not been applied since the tide gauge data do not have the pressure information to make a similar correction and GMSL is best computed from non-IB-corrected data since the average IB signal is zero but IB models often have a nonzero mean. The 1 s sea surface height measurements are interpolated to fixed bins along the ground track using a high-resolution mean sea surface model in order to account for geoid gradients [*Chambers et al.*, 1998]. Sea level anomalies (SLAs) in each bin are then computed by removing the time-averaged mean sea surface for that bin. The SLAs are averaged over months from January 1993 to December 1998 and gridded into 2.5° grids. Because there are still gaps in the grids and we desire to filter out shorter wavelength variations, the grids are smoothed with a Gaussian weighted filter described by *Chambers et al.* [1997]. The filter attenuates spatial signals of <1200 km zonally and 400 km meridionally.

[9] Since the focus of this research is on the low-frequency variability, the seasonal and semiannual signals have also been removed from the T/P grids by estimating sinusoids at annual and semiannual frequencies for each grid and removing them. We found that using the initial land mask reduced the number of tide gauges since most tide gauge sites are right on the coastline. In order to include more tide gauge data in the reconstruction, data up to one grid box (2.5°) inland from the coastline were given the value of the weighted average of the ocean values up to two grid boxes away (5°), where the weight was 1/distance. This allowed the determination of EOFs from the T/P grids at the sites of tide gauges, which is important in the procedure described in section 3.

[10] The tide gauge data are those collected by the Permanent Service for Mean Sea Level (PSMSL) [*Woodworth*, 1991]. We used the database updated in March 2000, which has substantial records through the end of 1998 (Figure 3). In order to use the tide gauge data for time series analysis the data at each site need to be reduced to a common datum. This is done at PSMSL by using the tide gauge datum history provided by the supplier of the tide gauge measurements. Approximately two thirds of the data in the PSMSL

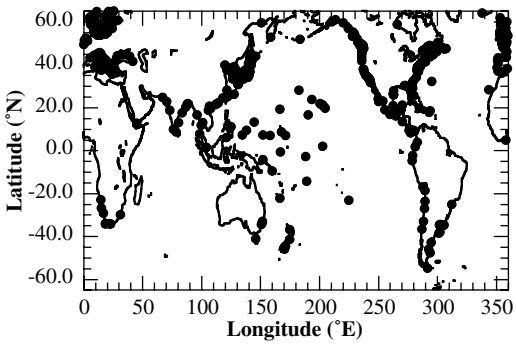

Figure 4. Location of tide gauge sites used in this investigation.

database have been adjusted this way and are referred to as the Revised Local Reference (RLR) data. The RLR data are considered superior to the data not reduced, so in this analysis, only RLR data are used.

[11] The RLR data also have arbitrary biases applied at each site of the order of 7000 mm in order to avoid negative numbers. Since we are interested in global sea level variability, this bias must be removed for all gauges relative to some consistent time period. In addition, as explained in section 3, secular trends are removed from the tide gauge data before calculating the EOF reconstruction. This has the benefit of reducing errors due to glacial isostatic adjustment or uplift/subsidence but also means that this analysis cannot measure secular rates of GMSL change, only low-frequency changes. Also, depending on the length of the tide gauge record, the removal of a trend could remove part of a long-period variation unrelated to secular change and thus remove true low-frequency variability. In order to mitigate this problem, only data with records longer than 25 years were used in this analysis. The locations of the sites used are shown in Figure 4. Figure 5 shows the number of records in years for each site after 1950. More than 81% of the sites have at least 30 years of observations, while more than 50% have 40 years or more of observations.

[12] In order to remove the bias, trend, and seasonal and semiannual signals the coefficients for a linear trend plus annual and semiannual sinusoids were estimated at each tide gauge location using least squares, and then the model was removed. All times were computed relative to an epoch of 1995.5 (the midpoint of the T/P data used) so that all data were reduced to SLAs relative to a similar mean sea level. Because there are sometimes several tide gauges in a particular 2.5° grid, we also averaged the residual tide gauge SLAs for each month into a 2.5° grid identical to the T/P data. The tide gauge data were averaged using a constant weight. This is done to reduce the effect of multiple observations of nearly identical sea level variability on the EOF reconstruction.

3. EOF Reconstruction

[13] The EOFs used in this research are obtained from a principal component analysis of the gridded T/P SLA data. The SLA data are formulated into an $m \times n$ matrix **H**, where m is the number of spatial grid points and n is the number of monthly grids. The matrix **H** is then separated into three matrices through a singular value decomposition of the data [*Preisendorfer*, 1988]:

$$\mathbf{H} = \mathbf{X}\Lambda\mathbf{P}, \tag{1}$$

where **X** is an $m \times n$ matrix whose columns form the EOFs of the decomposition, Λ is an $n \times n$ matrix whose diagonal values are the eigenvalues of **H**, and **P** is an $n \times n$ matrix whose rows represent the principal components associated with each EOF mode. The column vectors (EOFs) of **X** are orthogonal and form spatial maps of sea level variability. The rows of **P** are also orthogonal and provide the principal components describing the temporal variability of the EOFs. Each EOF is paired with a principal component to form n modes of ocean variability on the basis of the monthly grids of SLA data. The EOFs and principal components are ordered by the amount of variance of the total signal explained. Thus, the first mode will explain the largest percentage of variability, and the last modes will explain the least.

[14] The original T/P data can represented as a linear combination of the EOF modes and principal components [*Hendricks et al.*, 1996]:

$$\mathrm{SLA}(x,t) = \sum_{k=1}^{N} \alpha_k(x)\beta_k(t), \tag{2}$$

where x is the two-dimensional space domain, t is time, k is the EOF mode, N is the maximum number of modes used, $\alpha_k(x)$ is the kth column of **X** from (1) normalized by the maximum value, and $\beta_k(t)$ is the kth row of **P** from (1) scaled by the associated eigenvalue and the value used to normalize $\alpha_k(x)$. Thus, the sea level variations observed by T/P can be decomposed into maps of spatially correlated signals $\alpha_k(x)$ along with the associated time variations $\beta_k(t)$.

[15] For the EOF reconstruction technique described by *Smith et al.* [1996], gridded sparse data such as the tide gauge SLA are used as observations $O(x, t)$ and modern global data such as T/P are used to model spatial ocean variability $\alpha_k(x)$. Associated time variations $W_k(t)$ are estimated for each time step t and mode k to minimize

$$\varepsilon = O(x,t) - \left[\sum_{k=1}^{N} W_k(t)\alpha_k(x)\right] \tag{3}$$

using linear least squares estimation. For each month, N parameters will be estimated.

[16] Reconstructed grids $R(x, t)$ are computed on the basis of the estimated parameters (designated by angle brackets):

$$R(x,\ t) = \sum_{k=1}^{N} \langle W_k(t)\rangle \alpha_k(x). \tag{4}$$

Since $\alpha_k(x)$ is defined globally, the reconstructed grids will also be defined globally, unlike the sparse data that were used to estimate the coefficients $\langle W_k(t)\rangle$.

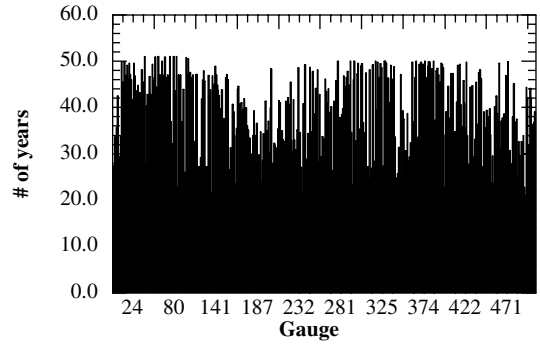

Figure 5. Number of observations (in years) for each tide gauge site. Tide gauge sites are numbered consecutively running from 0° to 360°E and 65°S to 65°N.

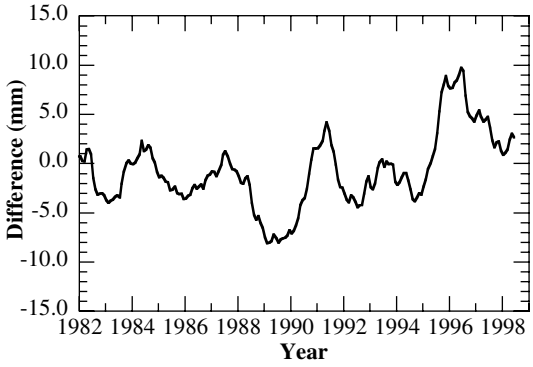

Figure 6. Difference between MSL estimated from tide gauge observations and SST EOFs from 1993 to 1998 and 1982 to 1998.

[17] The processing of the observations $O(x, t)$ in (3) needs to be discussed briefly. *Smith et al.* [1996] effectively recentered their observations every 10 years to have zero mean by removing a 10 year mean global grid from their gridded observations. The reconstruction was then performed on these recentered observations, although the decadal grids were added back in later. The main reason for this, as noted by *Kaplan et al.* [1997], is that time-varying biases (e.g., trends) in the observations will be projected onto the leading EOFs. Because the EOFs used as basis functions are computed over relatively short time intervals, true spatial patterns of GMSL change are not distinct in any one EOF mode [e.g., *Hendricks et al.*, 1996]. Therefore trends in the tide gauge observations will likely be projected erroneously onto the T/P EOF modes and lead to possible errors. Because of this, any recovered trends from the reconstruction would be suspect.

[18] There are an insufficient number of tide gauges to use the process utilized by *Smith et al.* [1996]. However, we do have long, nearly continuous, and reasonably well-calibrated measurements at the sites we are utilizing, so trends can be estimated and removed. This has the dual benefit of reducing the error from projecting trends to the EOF modes and removing unknown secular rates not associated with sea level change from the tide gauges. Therefore all our results are based on data and reconstructions with no long-term trends. The fact that the results do not have secular trends is an artifact of the analysis and should not be interpreted as an indication that sea level is not rising. Effectively, we have filtered the data to examine only long-term variations. If all gauges had only a maximum of 25 years of coverage, then one could not differentiate a signal with a period longer than 12–15 years from a longer-period signal. However, since half the gauges have more than 40 years of continuous observations, we believe that variations with periods up to 20–25 years can be distinguished. However, this investigation will focus on periods from 1 to 10 years.

[19] Note that although a long-term trend is removed from the tide gauge data, no trend is removed from the T/P data used to compute the EOF modes. This relates to the problem discussed in a previous paragraph, namely, that there is not a long enough time span of T/P observations to separate a long-term trend. Thus removing the trend from the T/P data is just as likely to remove an interannual period of 10 years as a true long-term trend. As more data from T/P and Jason 1 become available, this procedure will be able to be readdressed.

[20] *Smith et al.* [1996] also assumed that the EOF modes were stationary in time, so that modes computed with more recent data could be used to estimate principal components in the past. They present no proof of this assumption other than the fact that the reconstructed SST agrees well with withheld data. However, even if the modes are not stationary, the principal components could adjust in the estimation so that the summation in (4) still provides a reasonably accurate global grid. What this means is that the individual time series of the estimated principal components may have no physical meaning, but their use in (4) produces grids that are physically meaningful.

[21] One way to investigate the effect of assuming EOF modes are stationary is to reconstruct grids using the same observations but EOFs from different time spans. There are not enough T/P data to investigate the effect of using different time spans for calculating the basis EOF modes. Instead, we used EOFs from global SST data (1982–1998). We note that the SST EOF modes are significantly different from the SLA EOFs and that the reconstructed GMSL is very different and is not considered accurate. However, the test is useful to examine if statistics change over time. We computed EOFs from 1982 to 1998 and 1993 to 1998 and estimated principal components from the tide gauge observations from 1950 to 1998. The difference in the global averages is shown in Figure 6. The RMS before 1993 is not statistically different from the RMS after 1993 (and is actually slightly smaller), which suggests that the reconstructions estimated before 1993 should have errors similar to those computed after 1993, at least back to 1982.

[22] The analysis by *Smith et al.* [1996] used smaller regions for the EOF analysis (for example, the tropical Pacific), then combined the regions into a global map. We have tested this approach but found that the regions had to be fairly large in order to calculate reasonable reconstructed maps, on the basis of comparisons with T/P. However, it was found that using a global reconstruction produced maps closer to T/P than using even large regional reconstructions [*Chambers*, 2002]. For this reason we utilize global EOF maps from T/P and perform a global reconstruction each month.

[23] In addition to stationarity of EOF modes and the region over which the reconstruction is performed, the distribution of the tide gauge records in time may also affect the results. To examine the size of possible errors caused by this, we examined reconstructing maps using various distributions of tide gauges based on real data. Since the largest number of tide gauges was in the 1980s, this served as the baseline set. From this set we removed gauges until only those that had observed in earlier decades were included. For example, we examined each month in the 1960s. If a gauge observed for that month and the similar month in the 1980s, then the observation in the 1980s for that similar month were kept (e.g., January of 1961 compared to January of 1981). If there was no observation for a particular month in the 1960s, then the corresponding month in the 1980s for that gauge was likewise removed. This gave us sets of grids that contained approximately the same distribution of gauges for other decades but data from the 1980s. The distribution is approximate because there are cases where there were gauges in locations in earlier times but not in the 1980s. Thus the distribution actually tends to be more pessimistic than reality. In order to quantify the effect of the distribution the reconstruction was performed on the sampled sets of grids for each decade and compared to the results using all the gauges in the 1980s. The RMS differences of the GMSL estimated from the reconstructed grids are given in Table 1. The RMS values back to the 1950s are about the same, <1.5 mm. The result from the 1940s distribution is 2.3 mm. For earlier decades the difference is even larger (not shown). On the basis of this we concluded that GMSL could not be estimated

Table 1. Differences Caused by Tide Gauge Distribution

Decade	RMS Difference With 1980s Distribution, mm
1990s	1.3
1970s	1.2
1960s	1.2
1950s	1.5
1940s	2.3

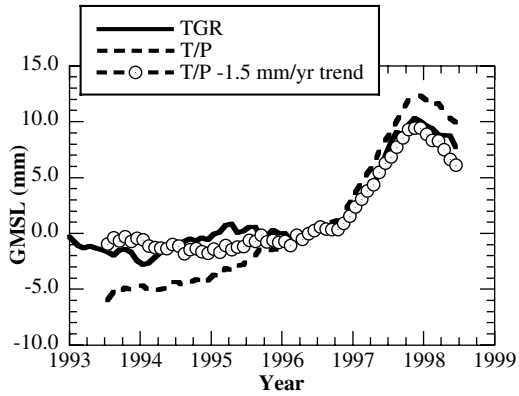

Figure 7. One year filtered GMSL from 1993 to 1998 for TGR, T/P, and T/P with a 1.5 mm yr^{-1} secular trend removed.

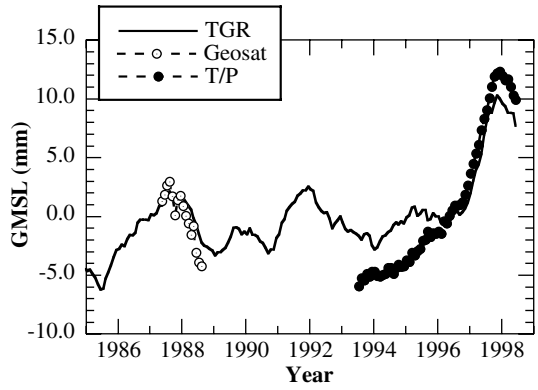

Figure 9. One year filtered GMSL from 1985 to 1998 for TGR, T/P, and Geosat.

accurately before 1950 using the distribution of tide gauges available.

[24] Also in this analysis, as in that of *Smith et al.* [1996], it has been assumed that all the observations have the same weight. We have experimented with weighting the tide gauge data using various factors, including the RMS difference of the tide gauge with T/P, the correlation with T/P, and the number of individual gauges going into each grid average. Minimal differences were found at interannual periods and longer [*Mehlhaff*, 2001]. Therefore, since many of the tide gauges do not have measurements at the same time as T/P and thus their weights would have to be estimated, we used weights of unity for all gridded tide gauge data. In the same study we experimented with adjusting N from 2 to 30 modes. It was found that the RMS difference of the sea levels measured by the tide gauge reconstruction and that of T/P improved significantly up to 10 modes but then leveled out with only minor changes. Because of this, we have used the first 10 EOF modes from the T/P data.

4. Results and Error Analysis

[25] GMSL change is computed from the gridded data as a weighted average, where the weight is cos(latitude). Since we are interested in only low-frequency variations, the time series have been further smoothed with a 13 month running mean boxcar filter. Figure 7 shows the GMSL time series for T/P and the tide gauge reconstruction (TGR) grids ($GMSL_{T/P}$ and $GMSL_{TGR}$) for the period 1993–1998. The agreement is good, with an RMS difference of 2.5 mm, mainly because the T/P GMSL is slightly higher at the end of the series and slightly lower at the beginning.

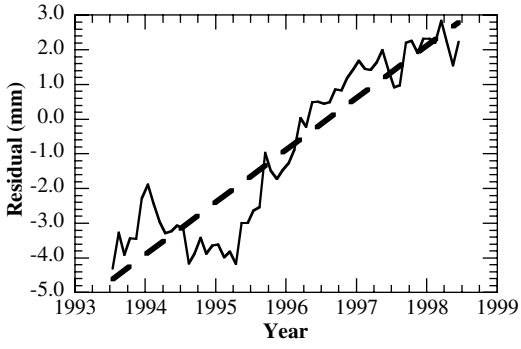

Figure 8. $GMSL_{T/P} - GMSL_{TGR}$ from Figure 7 (solid line). The dashed line is the best fit linear trend.

[26] We note again that long-term trends were removed from all the tide gauge records, but no trend was removed from the T/P data. Thus the T/P data will contain not only the low-frequency component of sea level change but the secular rate as well. Assuming $GMSL_{TGR}$ accurately represents the low-frequency variations, then the difference ($GMSL_{T/P} - GMSL_{TGR}$) would represent the secular rate of sea level change. The difference is shown in Figure 8 and is closely approximated by a linear trend with a slope of 1.5 ± 0.4 mm $year^{-1}$, which is in the middle of the generally accepted range of 1–2 mm yr^{-1} [*Church et al.*, 2001]. If a 1.5 mm yr^{-1} trend is removed from the T/P data, the resulting $GMSL_{T/P}$ time series (Figure 7) shows even better agreement with $GMSL_{TGR}$. The RMS difference is reduced to 1 mm from 2.5 mm.

[27] Although $GMSL_{TGR}$ agrees well with that from T/P, this could be because the EOF modes are determined by T/P. A better test of the method is to see if the reconstruction of older data has similar accuracy if EOF modes from that time period are not used. *Smith et al.* [1996] relied on over 10 years of data to compute their EOFs, but because of the shorter record of satellite altimetry, our basis EOFs rely on only 6 years of data. Therefore, to assess the accuracy of the $GMSL_{TGR}$ before 1993, other data sets have been used for comparison. The only other worthwhile global measure of sea level significantly before T/P is that made by the Geosat altimeter exact repeat mission from 1986 to 1989.

[28] We have used data from the recently reprocessed Geosat geophysical data records (GDRs) [*Lillibridge and Cheney*, 1997]. Only data during the exact repeat mission are utilized in this investigation. The new GDRs include new atmospheric, sea surface, instrument, and geophysical corrections that attempt to bring the Geosat data into standards consistent with T/P. Additionally, we have replaced the wet troposphere correction with that computed from the European Centre for Medium-Range Weather Forecasts (ECMWF) numerical model [*Urban et al.*, 2001] and have replaced the orbits with those computed using the Texas Earth Gravity model 3 (TEG-3) gravity field model [*Tapley et al.*, 1997]. Crossover statistics for the new orbits indicate a radial accuracy of 7–9 cm compared to 10 cm for the original orbit on the GDRs and 2–3 cm for T/P. Starting in the summer of 1988, the orbit accuracy for Geosat degrades to 15 cm or more. The orbit error appears to cause extreme changes in GMSL computed from Geosat after August 1988, so we use only data from November 1986 to August 1988 in this analysis. Complete details of the Geosat data processing are given by *Lillibridge and Cheney* [1997] and *Urban* [2000].

[29] SLAs are computed from the Geosat data similar to the processing for T/P; data are gridded into monthly maps, annual and semiannual signals are estimated and removed, and GMSL is calculated. Because the Geosat mission was not absolutely calibrated, the relative bias between the sea level measured by Geosat with that measured by T/P is not well known. Calibrations using

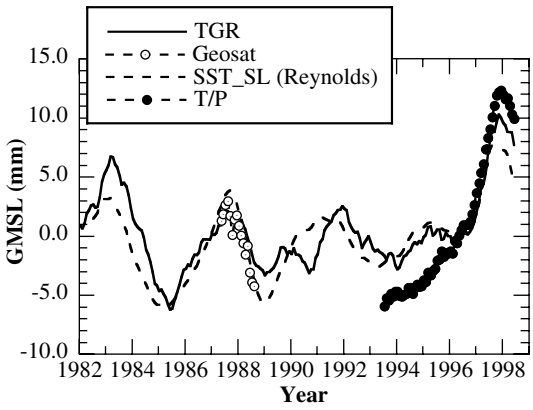

Figure 10. One year filtered GMSL from 1982 to 1998 for TGR, SST_SL from Reynolds SST, T/P, and Geosat.

tide gauges have been made [*Guman*, 1997; *Kruizinga*, 1997; *Urban*, 2000] but are only accurate to 2–3 cm. Since we are only interested in low-frequency variations and have already removed trends from the tide gauge data, we have simply removed the mean of the Geosat GMSL from our data so that it has zero mean.

[30] Figure 9 shows the filtered $GMSL_{Geosat}$ time series along with that for the TGR and T/P. Both the TGR and Geosat GMSL fall by about 5–6 mm from 1987 to late 1998, as the tropical Pacific shifted from an El Niño phase to a La Niña phase. The overall RMS between the TGR and Geosat curves (based on 16 samples) is 1.3 mm, which is comparable to the RMS with T/P. Although the Geosat data will also contain any secular change in GMSL change, the time span is so short that the total change would be <3 mm (assuming a rate of 1.5 mm yr^{-1}), and the statistics do not change significantly if an estimated trend is removed.

[31] Although the Geosat data suggest that the TGR is accurate at least back to 1986, the record is short. Therefore we have used other measurements to represent a proxy for sea level in order to determine additional statistics. Global SST has been shown to be correlated strongly with GMSL if seasonal variations in SST are first removed [*Nerem*, 1995; *Nerem et al.*, 1999; *Cabanes et al.*, 2001]. Correlation is poor when seasonal variations in SST are included because the thermal expansion of sea level is partly compensated for by seasonal variations in the global water cycle, which are out of phase [*Chen et al.*, 1998; *Minster et al.*, 1999]. For this research we have used global monthly maps of SST from two sources: SST from satellites for the period 1982–1998 optimally interpolated and calibrated by *Reynolds and Smith* [1994] and SST reconstructed from in situ measurements and modern EOFs for the period from 1950 to 1998 [*Smith et al.*, 1996]. These data sets will be referred to as the Reynolds SST and reconstructed SST, respectively. Both data sets were reaveraged into a 2.5° monthly grid identical to the grids used in this study, and the annual and semiannual variations were removed using estimated sinusoids. This should reduce differences due to the seasonal water cycle, although there is some evidence of interannual variations as well [*Chambers et al.*, 2000]. In addition, the linear trend from 1950 to 1998 for the reconstructed SST time series was estimated and removed to be consistent with the tide gauge processing of removing trends for periods longer than 25 years. The linear trend was not removed from the Reynolds SST grids in order not to remove variations with periods shorter than 25 years.

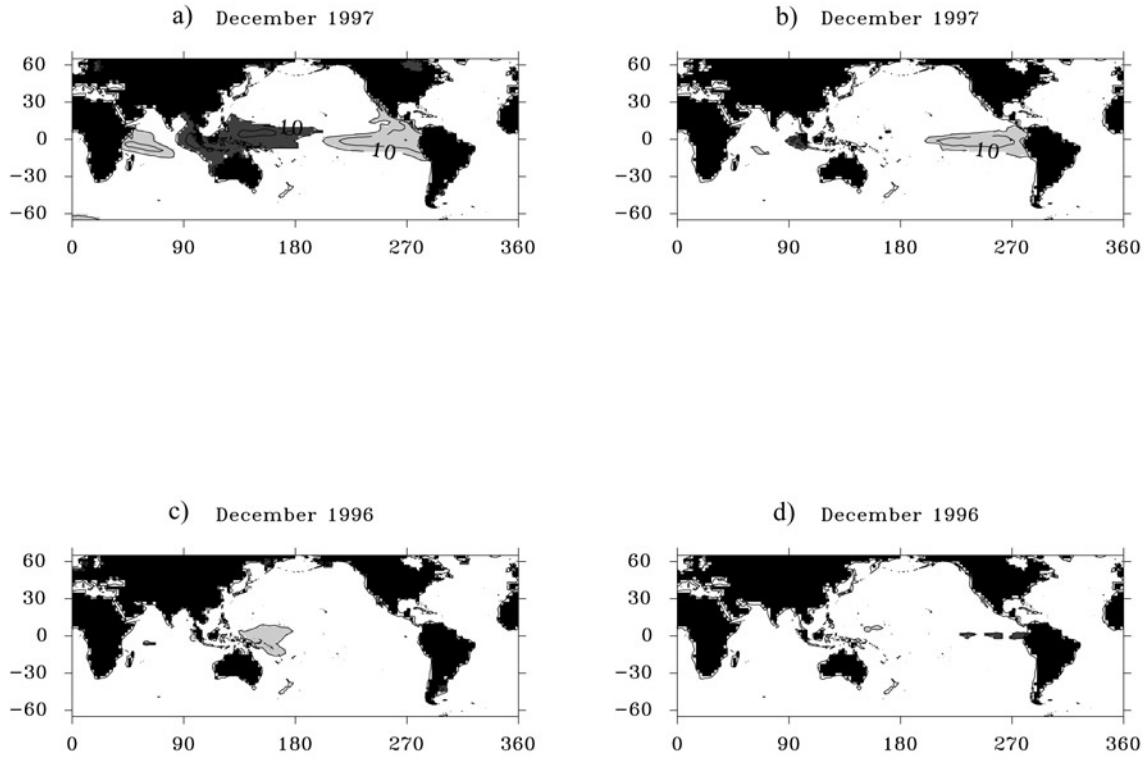

Figure 11. Maps of SLAs during an El Niño for (a) T/P and (b) SST_SL computed from Reynolds SST. Maps of SLAs during a La Niña for (c) T/P and (d) SST_SL.

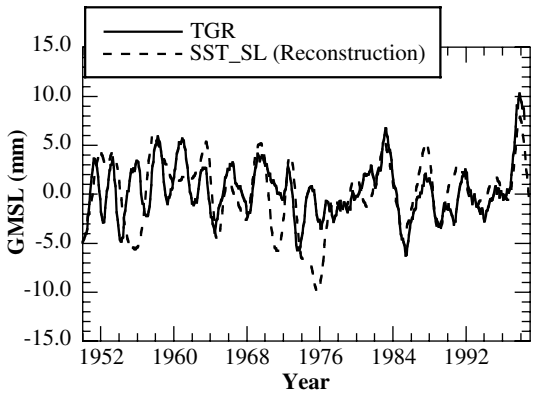

Figure 12. One year filtered GMSL from 1950 to 1998 for TGR and SST_SL from reconstructed SST.

[32] To convert the SST to a proxy sea level measurement, denoted SST_SL, the Reynolds SST data from 1993 to 1998 were regressed against T/P SLA in each grid by minimizing the function

$$\varepsilon = \mathrm{SLA}(x,\ t) - \left[a(x) + b(x)\mathrm{SST}\left(x,\ t + t_{lag}\right)\right] \qquad (5)$$

using least squares. The value x is the spatial location of the grid, t is the month, t_{lag} is the amount of time SST is shifted (up to ±4 months) to achieve maximum correlation, and $a(x)$ and $b(x)$ are parameters to estimate. The factor t_{lag} is used to account for the fact that SST and SLA are often slightly out of phase at certain locations. For example, heat flux at the air-sea interface can change SST, then mixing of the upper layer will change SLA some time later.

[33] The proxy SLA, SST_SL(x, t) is then calculated by using the estimated coefficients $\langle a(x)\rangle$ and $\langle b(x)\rangle$ and the true SST

$$\mathrm{SST\_SL}(x,t) = \langle a(x)\rangle + \langle b(x)\rangle \mathrm{SST}\left(x,\ t + t_{lag}\right). \qquad (6)$$

GMSL is then computed from the values for SST_SL(x, t). The coefficients estimated during the 1993–1998 period are used to regress the data in all the other periods, even for the reconstructed SST data. The results of the regression produce a proxy GMSL variation from 1982 to 1998 that agrees well with both T/P and Geosat GMSL in terms of phasing of interannual variations (Figure 10). More importantly, the comparison with $\mathrm{GMSL_{TGR}}$ during periods when there are no altimeter measurements shows a similar level of agreement.

[34] The proxy SST_SL is not meant to represent the true GMSL since the regression is based on the assumption that the SST anomalies are the same size and sign as the temperature anomalies below the surface and that the regression coefficient will not change in time. Instead, the SST_SL data are used to examine whether the $\mathrm{GMSL_{TGR}}$ variability is as similar to SST_SL before 1993 as it is after 1993. From 1982 to 1998 the GMSL from the TGR and the SST_SL data show similar ENSO variability, with peaks associated with El Niño in 1983, 1987, 1991–1992, 1994, and 1997. Both data sets also have similar troughs associated with La Niña in 1985, 1988, 1993, and 1996. The RMS difference from 1982 to 1992 is 2.1 mm, while the value from 1993 to 1998 is 1.5 mm. These values are comparable to RMS difference with T/P and Geosat (2.5 and 1.5 mm, respectively, when no estimated secular trends are removed).

[35] Note that although the phasings of the ENSO variations in GMSL and SST_SL are similar, the amplitude of the El Niño peaks is generally smaller in SST_SL than in GMSL (e.g., 1983 and 1997), while the La Niña troughs are larger (e.g., 1988 and 1993). If one examines the global maps from the SST_SL compared with "true" maps from T/P, an explanation for this is suggested (Figure 11). As discussed by *Nerem et al.* [1999] regarding sea level and *White et al.* [2001] investigating ocean heat storage, variability in the tropical Pacific associated with ENSO has the largest effect on global means for interannual timescales. Figures 11a and 11b show that the SST_SL data underestimate the amplitude and area of the positive SLA in the eastern Pacific compared to T/P and also severely underestimate a correlated variation in the western Indian Ocean. The regression in the western Pacific is even more problematic because although the SST variation is small, the sea level variation is large as the thermocline depth adjusts in this region during ENSO. Thus, during La Niña phases (Figures 11c and 11d) the SST_SL maps do not indicate the large increase in sea level in the western Pacific that is observed by altimetry and tide gauges. Because of this, we suspect GMSL computed from the SST_SL data will be biased more negative during La Niña and would also not accurately reflect the true amplitude during El Niño.

[36] This is also observed when the GMSL from the TGR is compared with SST_SL determined from reconstructed SST (Figure 12). The RMS difference from 1970 to 1980 is 4.1 mm, which is significantly larger than the RMS after 1982. However, we note that the difference is mainly caused by the two large La Niña episodes in 1970 and in 1976. The RMS difference before 1970 is also 3–4 mm, mainly because the TGR data appear to contain more cyclical ENSO cycles than the SST_SL data. One interesting difference occurs in 1956, when the SST_SL indicates a GMSL drop, which is at the same time as a La Niña as indicated by the Southern Oscillation Index (Figure 15). However, the TGR indicates an increase in GMSL at that time.

[37] On the basis of these statistics we assign an error of ±2 mm from 1980 to 1998 for the GMSL from TGR with 1 year filtering. This is based on the RMS difference with T/P and Geosat and the fact that the SST_SL comparisons have similar RMS values between 1980–1992 and 1993–1998. Note that the 2 mm value is about 1σ compared to T/P if one does not account for a model of long-term GMSL change but is 2σ if one does (e.g., Figure 7). Before 1980 we assign an error of ±4 mm since the comparisons with the SST_SL are about twice as large. This may be slightly conservative because of the problems in SST_SL noted earlier.

[38] In addition to the 1 year filtering, we have also filtered the GMSL time series with a 5 year running mean boxcar (Figure 13). Ignoring the large difference in the 1970s caused by the La Niña bias in the SST_SL, the GMSL time series all show remarkable agreement in phase and amplitude. The RMS difference statistics are 0.6 mm for 1982–1998, 2.2 mm for 1970–1979 (including the bias effect), and 0.8 mm for 1950–1969. On the basis of this we

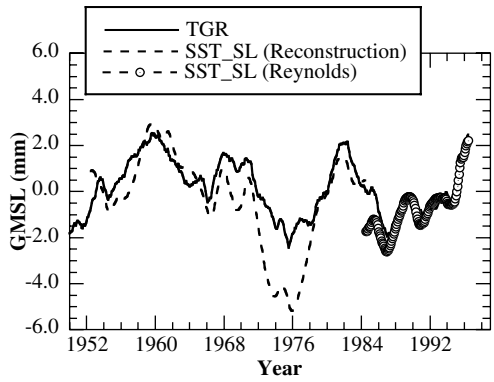

Figure 13. Five year filtered GMSL from 1950 to 1998 for TGR, SST_SL from reconstructed SST, and SST_SL from Reynolds SST.

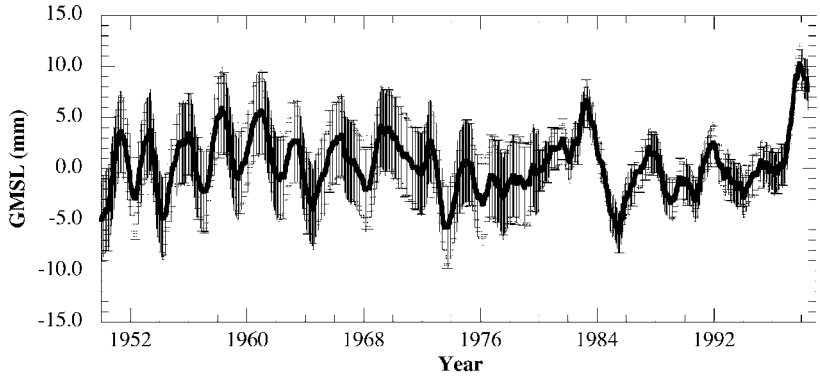

Figure 14. One year filtered GMSL from 1950 to 1998 for TGR with estimated error bars.

assign a constant error of ±1 mm to the 5 year filtered GMSL time series from the TGR.

5. Discussion of Results

[39] Figure 14 shows the 1 year filtered GMSL from the TGR along with its estimated error bars. There are significant variations that are generally correlated with El Niño and La Niña episodes, as determined from the Southern Oscillation Index (SOI) (Figure 15). During the ~50 year period, there were 10 El Niño events (maxima) and 9 La Niña episodes (minima) where the SOI exceeded 1σ. Within 4 months of each maximum defined by the SOI, there were significant peaks in GMSL for 8 of these events. In 7 of the 8 the SOI peak led the GMSL peak. During five of the strong La Niña episodes the GMSL had a significant minima. This suggests that the findings from the T/P measurements that GMSL rises during or just after El Niño [*Nerem et al.*, 1999] is not unique to that time period but has occurred at other times. The TGR data also indicate that there is generally a significant drop in GMSL associated with La Niña.

[40] The size of the SOI does not necessarily predict the magnitude of the change in GMSL, and there are also a few times

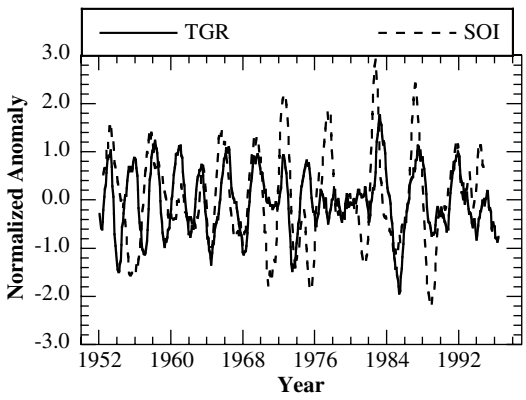

Figure 15. Normalized anomalies of GMSL from TGR and Southern Oscillation Index (SOI). The normal SOI has been multiplied by a factor of −1 in order that El Niño events have positive values. Both time series have been filtered with the same 13 month running mean boxcar filter and the 5 year running mean values have been removed in order to isolate interannual events. The values plotted are SOI divided by standard deviation of SOI and GMSL divided by estimated error (4 mm for 1950–1980 and 2 mm for 1980–1998).

when GMSL appears to change in a way uncorrelated with ENSO. For example, from 1953 to 1956 the SOI indicates a single shift from El Niño to La Niña, whereas the GMSL indicates nearly two complete cycles in the same period, with a significant positive SLA during the La Niña of 1955. In 1971 a large La Niña is indicated by the SOI, but only a small, insignificant drop in GMSL is observed. From 1976 to 1978 the SOI suggests a shift from La Niña to El Niño, while the GMSL has insignificant variability.

[41] These differences most likely occur because the SOI does not always fully represent the large-scale ENSO cycle, because the GMSL error is not necessarily random and may be correlated with ENSO cycles, and because factors other than ENSO also effect GMSL. Still, the large number of positive correlation values is significant and suggests that the ENSO climate variability does significantly affect GMSL as a rule.

[42] With 5 year filtering, Figure 16 shows the significant low-frequency variations in GMSL from 1950 to 1998. These results indicate GMSL was significantly lower than normal in the early 1950s, 1970s, and late 1980s and was higher than normal in the early 1960s, early 1980s, and late 1990s. As noted before, these variations have also been observed in global averages of SST data. The GMSL has also been compared with an index of the low-frequency climate variation known as the Pacific Decadal Oscillation (PDO) [*Mantua et al.*, 1997] (Figure 17). The GMSL is well correlated with the PDO, suggesting that GMSL is higher than normal during "warm" phases of the PDO (positive indices) and lower than normal during "cool" phases. During warm phases of PDO the eastern tropical Pacific is generally warmer than normal while the northwestern and southwestern Pacific are cooler than normal. During a cool phase the modes reverse. The GMSL is not perfectly correlated with the PDO, so there are clearly other forcings besides ENSO and PDO on the GMSL.

[43] We have examined the North Atlantic Oscillation as well but have found no significant correlation with the TGR GMSL. Note that the correlation is strong with the PDO even though there are significantly more gauges in the North Atlantic than in the Pacific (Figures 3 and 4). This may be due to the fact that variations in the Pacific tend to be larger than those in the Atlantic and the area is larger. It is unclear whether this correlation is an artifact of the EOF reconstruction because of this, so more work needs to be done to quantify this.

[44] One effect of interannual and low-frequency variations in GMSL is that estimates of secular trends cannot be accurately calculated from short records of altimetry data. *Nerem et al.* [1999] attempted to model how much altimetry data is necessary to estimate a 2 mm yr^{-1} rise in sea level given the presence of ENSO-like variability. They found it would take at least 10 years to estimate the trend to an accuracy of 0.5 mm yr^{-1}. We have repeated this simulation using the time series of low-frequency

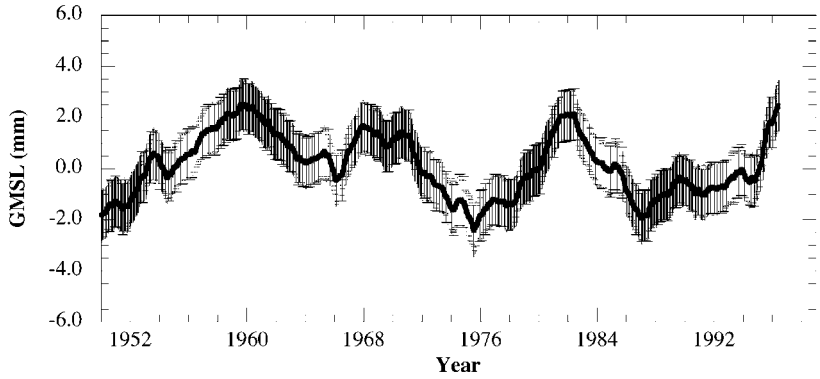

Figure 16. Five year filtered GMSL from 1950 to 1998 for TGR with estimated error bars.

GMSL variations and find that it also suggests a 10 year period is necessary. If the accuracy requirement is tightened to 0.25 mm yr^{-1}, we find a 12–15 year period is needed.

[45] Note that the T/P measurements are being made during what appears to be the increasing portion of one of these decadal oscillations. Although the recent data from T/P indicate a decrease in GMSL after 1998, it still may take longer than 10–15 years to recover a true secular trend with the desired accuracy. Hence it is important to continue the altimeter measurement of GMSL after T/P as there are currently no other methods to measure the true global secular trend in GMSL change. However, maintaining the tide gauge network is equally important in order to examine the even longer interdecadal variability of global mean sea level and its variability over the past 100 years. While altimetry is expected to monitor interdecadal variability for the foreseeable future, only tide gauge records will be able to tie current and future variations to past variability.

6. Conclusions

[46] Tide gauge records back to 1950 have been used to reconstruct a time series of GMSL that is estimated to have an accuracy of 2–4 mm RMS for 1 year filtering and 1 mm RMS for 5 year filtering. The accuracy is estimated from statistical comparisons with altimeter and proxy sea level measurements. The GMSL has significant variations correlating to El Niño and La Niña cycles and the Pacific Decadal Oscillation for periods longer than 5 years over the past 50 years.

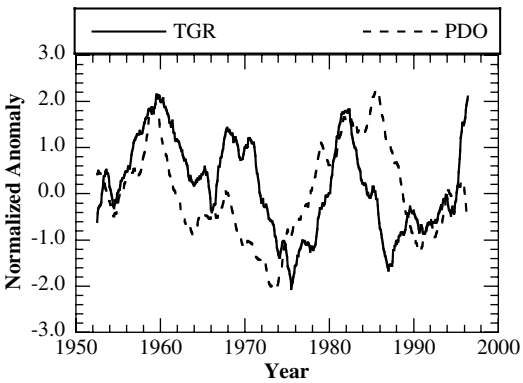

Figure 17. Normalized anomalies of GMSL from TGR and index of Pacific Decadal Oscillation (PDO). Both time series have been filtered with the same 60 month running mean boxcar filter. The values plotted are PDO index divided by standard deviation of PDO index and GMSL divided by standard deviation of GMSL.

[47] The GMSL time series from the TGR presented here cannot be used to determine the long-term secular rate of sea level change since the tide gauge data have had linear trends removed. However, if the TGR represents the true low-frequency GMSL in the absence of secular trends, then it can be differenced with GMSL computed from altimetry in order to determine the residual secular trend. Assuming this is the case, then removing the TGR from T/P implies a rate of 1.5 ± 0.4 mm yr^{-1}, similar to the rate estimated directly from tide gauge data without accounting for the sampling. In addition, the GMSL time series from the TGR can be used to estimate how much altimeter data alone may be necessary to measure the rate. Our calculations indicate 10 years will be necessary to recover the rate to within ±0.5 mm yr^{-1}, and 12–15 years will be necessary to recover the rate to within ±0.25 mm yr^{-1}.

[48] We have examined reconstructing global maps for the period before 1950. As Figure 3 indicates, there are few tide gauges in the tropical Pacific at that time. Because GMSL appears to be related strongly to ENSO and the PDO, any reconstruction of GMSL is considered suspect without sufficient data in the tropical Pacific, and the probable error is much larger than the signal. However, the amount of data in the Atlantic basin may be sufficient to examine low-frequency variations in that basin as far back as 1900 and perhaps even earlier.

[49] When more altimeter data is available in the future, we can also begin to examine more closely whether the EOF modes are stationary, and if not, how much of an effect this may have on the solution. There are also undoubtedly systematic errors in the procedure that are difficult to determine. For example, it is likely that the error is larger during certain periods than at others. More work needs to be done to quantify this, and additional altimetry may help with this. In addition, after 10–15 years of altimeter data we may be able to separate an EOF mode that contains most of the secular trend signal. If this is the case, we might be able to reconstruct the GMSL time series from the TGR data without removing secular trends. In some simple experiments we found that we were able to recover a realistic secular trend in the reconstruction if a mode was included that contained the spatial pattern of secular rise/fall of sea level. However, the rate could not be recovered if an incorrect pattern was used. At this point the model used to correct for GIA is important, as is the effect of other geophysical processes isolated to land.

[50] **Acknowledgments.** TOPEX/Poseidon data are from the Physical Oceanography Data Archive Center at Jet Propulsion Laboratory/California Institute of Technology. Geosat data are from the National Oceanographic and Atmospheric Administration (NOAA) National Oceanographic Data Center. Tide gauge data are from Permanent Service for Mean Sea Level. SST data are from the optimal analysis by Richard Reynolds and Thomas Smith at the NOAA Climate Diagnostics Center. The Southern Oscillation Index was calculated by the National Centers for Environmental Prediction (NCEP) Climate Prediction Center. The Pacific Decadal Oscillation index

was calculated by Nate Mantua. This research was supported by the Solid Earth Natural Hazards Program at NASA under grant NAG5-9144 and by the Jason 1 project at the NASA Jet Propulsion Laboratory under grant JPL-1226830. Locations of data sources on the Internet are ftp://ftp.ncep.noaa.gov/pub/cpc/wd52dg/data/indices/soi (SOI), ftp://ftp.atmos.washington.edu/mantua/pnw_impacts/INDICES/PDO.latest (PDO), http://www.nbi.ac.uk/psmsl/datainfo (PSMSL tide gauge data), http://www.cdc.noaa.gov/cdc/data.reynolds_sst.html (Reynolds SST), and http://www.cdc.noaa.gov/cdc/data.recon_reynolds_sst.html (reconstructed SST).

References

Benada, R., TOPEX/Poseidon merged GDR generation B user's handbook, *JPL Rep. D-11007*, Jet. Propul. Lab., Pasadena, Calif., 1997.

Born, G. H., B. D. Tapley, J. C. Ries, and R. H. Stewart, Accurate measurement of mean sea level changes by altimetric satellites, *J. Geophys. Res.*, *91*, 11,775–11,782, 1986.

Cabanes, C., A. Casenave, and C. Le Provost, Sea level change from TOPEX-Poseidon Altimetry for 1993–1999 and possible warming of the Southern Ocean, *Geophys. Res. Lett.*, *28*, 9–12, 2001.

Cane, M. A., A. Kaplan, R. N. Miller, B. Tang, E. C. Hackert, and A. J. Busalacchi, Mapping tropical Pacific sea level: Data assimilation via a reduced state space Kalman filter, *J. Geophys. Res.*, *101*, 22,599–22,618, 1996.

Cazenave, A., K. Dominh, M. C. Gennero, and B. Ferret, Global mean sea level changes observed by TOPEX-Poseidon and ERS-1, *Phys. Chem. Earth*, *23*, 1069–1075, 1998.

Chambers, D. P., Seasonal and low-frequency variability in global and basin-scale sea level, *J. Geodesy*, in press, 2002.

Chambers, D. P., B. D. Tapley, and R. H. Stewart, Long-period ocean heat storage rates and basin-scale heat fluxes from TOPEX, *J. Geophys. Res.*, *102*, 10,525–10,533, 1997.

Chambers, D. P., B. D. Tapley, and R. H. Stewart, Reduction of geoid gradient error in ocean variability from satellite altimetry, *Mar. Geod.*, *21*, 25–39, 1998.

Chambers, D. P., J. L. Chen, R. S. Nerem, and B. D. Tapley, Interannaul sea level change and the Earth's water mass budget, *Geophys. Res. Lett.*, *27*, 3073–3076, 2000.

Chen, J. L., C. R. Wilson, D. P. Chambers, R. S. Nerem, and B. D. Tapley, Seasonal global water mass balance and mean sea level variations, *Geophys. Res. Lett.*, *25*, 3555–3558, 1998.

Church, J. A., et al., Changes in sea level, in *Climate Change 2001, The Scientific Basis: Contribution of Working Group 1 to the Third Assessment Report of the Intergovernmental Panel on Climate Change*, edited by J. T. Houghton et al., pp. 639–694, Cambridge Univ. Press, New York, 2001.

Douglas, B. C., Sea level change in the era of the recording tide gauge, in *Sea Level Rise: History and Consequence*, edited by B. C. Douglas, M. Kearney, and S. Leatherman, pp. 37–64, Academic, San Diego, Calif., 2001.

Fu, L. L., E. J. Christensen, C. A. Yamarone Jr., M. Lefebvre, Y. Ménard, M. Dorrer, and P. Escudier, TOPEX/Poseidon mission overview, *J. Geophys. Res.*, *99*, 24,369–24,381, 1994.

Guman, M. D., Determination of global mean sea level variations using multi-satellite altimetry, *Rep. CSR-97-3*, Cent. for Space Res., Austin, Tex., 1997.

Hendricks, J. R., R. R. Leben, G. H. Born, and C. J. Koblinsky, Empirical orthogonal function analysis of global TOPEX/Poseidon altimeter data and implications for detection of global sea level rise, *J. Geophys. Res.*, *101*, 14,131–14,146, 1996.

Kaplan, A., Y. Kushnir, M. A. Cane, and M. B. Blumenthal, Reduced space optimal interpolation of historical data sets: 136 years of Atlantic sea surface temperature, *J. Geophys. Res.*, *102*, 27,835–27,860, 1997.

Kaplan, A., Y. Kushnir, and M. A. Cane, Reduced space optimal interpolation of historical marine sea level pressure: 1854–1992, *J. Clim.*, *13*, 2987–3002, 2000.

Keihm, S. J., V. Zlotnicki, and C. S. Ruf, TOPEX microwave radiometer performance evaluation, *IEEE Trans. Geosci. Remote Sens.*, *38*, 1379–1386, 2000.

Kruizinga, G. L. H., Validation and application of radar satellite altimetry, *Rep. CSR-97-6*, Cent. for Space Res., Austin, Tex., 1997.

Lillibridge, J., and R. Cheney, The Geosat altimeter JGM-3 GDRs on CD-ROM, Lab. For Satell. Imagery, Natl. Oceanogr. Data Cent., Silver Spring, Md., 1997. (Available at http://ibis.grdl.noaa.gov/SAT/gdrs/geosat_handbook/index.html.)

Mantua, N. J., S. R. Hare, Y. Zhang, J. M. Wallace, and R. C. Francis, A Pacific interdecadal climate oscillation with impacts on salmon production, *Bull. Am. Meteorol. Soc.*, *78*, 1069–1079, 1997.

Mehlhaff, C. A., Reconstructing sea level change from tide gauges and empirical orthogonal functions derived from TOPEX/Poseidon altimetry, *Tech. Memo. CSR-TM-00-07,* Cent. for Space Res., Austin, Tex., 2001.

Minster, F. F., C. Brossier, and P. Rogel, Variation of the mean sea level from TOPEX/Poseidon data, *J. Geophys. Res.*, *100*, 25,153–25,162, 1995.

Minster, J. F., A. Cazenave, Y. V. Serafini, F. Mercier, M. C. Gennero, and P. Rogel, Annual cycle in mean sea level from TOPEX-Poseidon and ERS-1: Inference on the global hydrological cycle, *Global Planet. Change*, *20*, 57–66, 1999.

Nerem, R. S., Measuring global mean sea level variations using TOPEX/Poseidon altimeter data, *J. Geophys. Res.*, *100*, 25,135–25,151, 1995.

Nerem, R. S., D. P. Chambers, E. Leuliette, G. T. Mitchum, and B. S. Giese, Variations in global mean sea level during the 1997-98 ENSO event, *Geophys. Res. Lett.*, *26*, 3005–3008, 1999.

Preisendorfer, R. W., *Principal Component Analysis in Meteorology and Oceanography*, edited by C. Mobley, 418 pp., Elsevier Sci., New York, 1988.

Reynolds, R. W., and T. M. Smith, Improved global sea surface temperature analysis using optimum interpolation, *J. Clim.*, *7*, 929–948, 1994.

Shen, S. S. P., G. R. North, and K. Y. Kim, Spectral approach to optimal estimation of the global average temperature, *J. Clim.*, *7*, 1999–2007, 1994.

Shriver, J. F., and J. J. O'Brien, Low-frequency variability of the equatorial Pacific Ocean using a new pseudostress dataset: 1930–1989, *J. Clim.*, *8*, 2762–2786, 1995.

Smith, T. M., R. W. Reynolds, R. E. Livezey, and D. C. Stokes, Reconstruction of historical sea surface temperatures using empirical orthogonal functions, *J. Clim.*, *9*, 1403–1420, 1996.

Tapley, B. D., C. K. Shum, J. C. Ries, R. Suter, and B. E. Schutz, Monitoring of changes in global mean sea level using Geosat altimeter, in *Sea Level Changes: Determination and Effects*, *Geophys. Monog. Ser.*, vol. 69, edited by P. Woodworth, pp. 167–180, AGU, Washington, D. C., 1992.

Tapley, B. D., et al., The TEG-3 geopotential model, in *Gravity, Geoid, and Marine Geodesy*, edited by J. Seagwa, H. Fujimoto, and S. Okubo, pp. 453–460, Springer-Verlag, New York, 1997.

Urban, T. J., The integration and application of multi-satellite radar altimetry, *Rep. CSR-00-01,* Cent. for Space Res., Austin, Tex., 2000.

Urban, T. J., T. Pekker, B. D. Tapley, G. L. H. Kruizinga, and C. K. Shum, A multiyear intercomparison of wet troposphere corrections from TOPEX/Poseidon, ERS-1, and ERS-2 Microwave Radiometers and the European Centre for Medium-Range Weather Forecasts model, *J. Geophys. Res.*, *106*, 19,657–19,669, 2001.

Wagner, C. A., and R. E. Cheney, Global sea level changes from satellite altimetry, *J. Geophys. Res.*, *97*, 15,607–15,615, 1992.

White, W. B., D. R. Cayan, M. D. Dettinger, and G. Auad, Sources of global warming in upper ocean temperature during El Niño, *J. Geophys. Res.*, *106*, 4349–4367, 2001.

Woodworth, P. L., The permanent service for mean sea level and the global sea level observing system, *J. Coastal Res.*, *7*, 699–710, 1991.

D. P. Chambers, D. Fujii, C. A. Mehlhaff, and T. J. Urban, Center for Space Research, University of Texas at Austin, Austin, TX 78759-5321, USA. (chambers@csr.utexas.edu)

R. S. Nerem, Colorado Center for Astrodynamics Research, University of Colorado at Boulder, Boulder, CO 80309, USA.